Supplementary Method

Traditional Features of Magnetic Resonance Imaging (MRI)

The traditional quantitative features included:

(1) Lesion size: maximum dimension measured on the coronal or axial plane on hepatobiliary phase (HBP) images;

(2) Apparent diffusion coefficient (ADC; b=800 s/mm2) value;

(3) HBP signal intensity (SI);

(4) T1 value (T1N) and T1 reduction rate (T1D): T1N refers to T1 relaxation time of tumor in the T1 mapping images before enhancement, and T1E is defined as T1 relaxation time after 20 minutes of injection of contrast agent, then T1D is equal to (T1N-T1E)/T1N.

The traditional qualitative MRI features included:

(1) Tumor margin: evaluated on coronal or axial HBP images, and divided into four types: smooth single nodular (type I), nodular with perinodular extension (type II), polynodular fusion (type III), and infiltrative (type IV);

(2) Dynamic enhanced pattern: arterial phase hyperenhancement and non-peripheral washout, continuous enhancement, delayed enhancement, no or slight enhancement;

17 (3) Abnormal peritumoral perfusion on arterial phase: irregular and patchy peritumoral

18 hyperenhancement on the arterial phase that became isointense with normal liver parenchyma

19 in later dynamic phases;

20 (4) Tumor vessels on the arterial phase: visible intratumor blood vessel on the arterial phase;

21 (5) Rim enhancement on the arterial phase: ring-like enhancement with central relative

22 hypointensity;

23 (6) SI on the arterial phase compared to normal liver parenchyma;

24 (7) Peritumoral hypointensity on HBP images: irregular or wedge-shaped hypointense areas

25 around the tumor on HBP images;

26 (8) Target signs on HBP/diffusion-weighted imaging (DWI; b = 800 s/mm2): ring-like high SI

27 with central relative hypointensity;

28 (9) Intratumoral cystic portion or necrosis: defined as high SI areas inside the lesion on T2-

29 weighted imaging (T2WI) or low SI areas not enhanced during dynamic enhancement;

30 (10) Intratumoral hemorrhage: high SI on T1-weighted imaging (T1WI) with variable SI on T2WI;

31 (11) Fat content: compared with the in-phase images, the tumor area had decreased SI on out-

32 phase images;

33 (12) Tumor capsule: smooth, uniform, sharp border around most or all of the tumor, visible as

34 an enhancing rim in the portal phase or transition phase;

35   (13) Vessel invasion (including blood vessels and bile ducts) or lymph node metastasis;

36   (14) Intratumoral septum: delayed enhanced strain-like septum could be seen in the portal

37   phase or transition phase

38
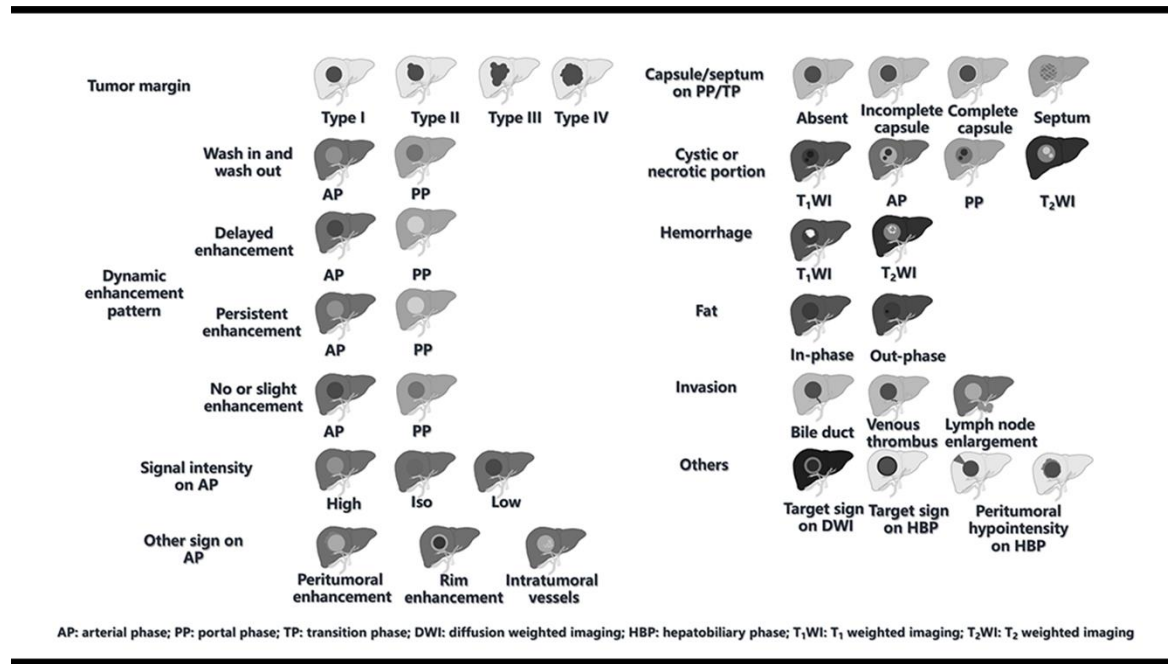
39   **Supplementary Figure 1.** Schematic Diagram of Gadoxetic Acid-enhanced Magnetic

40   Resonance Imaging Findings

41

42   *Image preprocessing*

43   Before the CT data were fed into the segmentation network, image preprocessing included

44   normalization, radiologist intervention, and data augmentation were performed as follows: (a)

45   Normalization: The CT values of the images were set between -120 HU and 230 HU, and then

46   all original intensities were normalized to decrease the data variance. (b) Radiologist

47   intervention: To improve the segmentation performance, the lesion of each patient was

48   identified by radiologists who used three-dimensional rectangular boxes (region of interest, ROI)

49   to completely enclose the area of the tumor. All transverse slices in each ROI were used as

50   input to the segmentation network. (c) Data augmentation: A deep learning (DL) network usually

51   requires a large amount of input data to train a model satisfactorily to avoid overfitting. We

52   solved this problem by augmenting the training dataset by horizontal mirroring, image rotating,

53   and image scaling.

54   Before the HBP images were fed into the segmentation model for semantic feature

55   extraction, image preprocessing was also performed as follow: (a) Normalization: To speed up

56   the gradient descent and search for the optimal solution, we perform a min-max normalization

57   of the original data. (b) Radiologist intervention: The lesion of each patient was identified by

58   radiologists who used ROI to completely enclose the area of the tumor. All transverse slices in

59   each ROI were used as input to the segmentation network. (c) Resampling: The voxel size of

60   all images was resampled to 0.5 mm × 0.5 mm × 1.0 mm using bicubic interpolation.

61

62   *Training strategy of segmentation network*

63   U-Net is a typical encoder–decoder structure in DL. In our study, the U-Net network was

64   used for segmentation tasks. The network was composed of two parts, encoder and decoder,

65   and the connection between encoding and decoding was realized by skipping connection. In

66   the training of this segmentation network, the cross-entropy loss was adopted and the

67 convolutional neural network segmentation network was optimized using Adam with the

68 following parameters: basic learning rate=1×10−4; iteration=50,000. The entire training

69 procedure took approximately 10 hours. The best segmentation model was selected by the dice

70 coefficient on the validation set. The dice coefficient is calculated as

71 $$DSC = \frac{2|A \cap B|}{|A|+|B|} \qquad (1)$$

72 where A and B are the ground truth and the predicted segmentation mask of the tumor,

73 respectively.

74

Supplementary Tables

Supplementary Table 1 MR scan sequence and parameters

sequence	Orientation	Category	TR/ms	TE/ms	FOV	Matrix	Thick-ness/ mm	Band width/ (Hz/Px)	Reverse angle
Magneton Trio A Tim 3.0T system (Siemens Healthcare Sector, Erlangen, Germany)									
T_2WI	TRA	TSE	2 000	81	328×350	240×320	5	260	150°
T_1WI IN/OUT PHASE	TRA	FLASH	200	2.2/1.1	328×350	192×256	6	930/977	65°
DWI	TRA	EPI	5 100	73	360×288	192×154	5	2 004	/
T_1mapping	TRA	VIBE	3.37	1.18	328×350	256×204	3	500	2/11°
T_1WI-FS Contrast-enhanced	TRA	VIBE	3.3	1.2	328×350	128×256	2	501	13°
T_1WI	TRA/ COR	VIBE	3.3	1.2	328×350	128×256	2	501	13°
T_1mapping	TRA	VIBE	3.37	1.18	328×350	256×204	3	500	2/11°
T_1WI （HBP）	TRA/ COR	VIBE	3.3	1.2	328×350	154×256	2	501	13°
GE 3.0T (750W, Pioneer) MR scanning system									
T_2WI	TRA	TSE	2000	81	328×350	320×224	5	260	150°
T_1WI IN/OUT PHASE	TRA	FLASH	200	2.2/1.1	328×350	320×208	4	930/977	65°
DWI	TRA	EPI	5 100	73	360×288	128×128	5	2 004	/
T_1WI-FS Contrast-enhanced	TRA	LAVA	3.3	1.2	328×350	320×208	4	501	13°
T_1WI	TRA/ COR	LAVA	3.3	1.2	328×350	320×208	4	501	13°
T_1WI （HBP）	TRA/ COR	LAVA	3.3	1.2	328×350	320×208	4	501	20°

77

78   **Supplementary Table 2** Laboratory indicators and reference range

Laboratory indicatiors	Abbreviations	UNIT	Reference range
Alanine amino transferase	*ALT*	U/L	1-40
Aspartic transaminase	*AST*	U/L	1-37
Total bilirubin	*TBIL*	umol/L	3-20
Albumin	*ALB*	g/L	35-50
Prothrombin time	*PT*	s	11-14
alpha fetoprotein	*AFP*	ug/L	0-20
Carbohydrate antigen 19-9	*CA19-9*	U/ml	0-35

79

80   **Supplementary Table 3** Univariate analyses of clinical characteristics in the training set

Variables	CK19+ (n=25)	CK19-(n=77)	Statistics (t/$\chi2$)	*P*
age/y	53±14	54±12	0.585	0.369
Sex			0.792	0.374
male	22（88.0）	72（93.5）		
female	3（12.0）	5（6.5）		
History of hepatitis B			0.792	0.374
yes	22（88.0）	72（93.5）		
no	3（12.0）	5（6.5）		
Child-pugh class			2.969	0.085
A	23（92.0）	76（98.7）		
B	2（8.0）	1（1.3）		
ALT (U/L)			1.298	0.255
>40	6（24.0）	28（36.4）		
≤40	19（76.0）	49（63.6）		
AST (U/L)			0.026	0.871

Variables	CK19+ (n=25)	CK19-(n=77)	Statistics (t/χ2)	P
>37	8 (32.0)	26 (33.8)		
≤37	17 (68.0)	51 (66.2)		
TBIL (umol/L)			1.113	0.291
>20	7 (28.0)	14 (18.2)		
≤20	18 (72.0)	63 (81.8)		
ALB (g/L)			0.572	0.449
<35	4 (16.0)	8 (10.4)		
≥35	21 (84.0)	69 (89.6)		
PT (s)			/	1.000
>14	0 (0.0)	1 (1.3)		
≤14	25 (100.0)	76 (98.7)		
AFP (ug/L)			9.876	0.002*
>400	12 (48.0)	13 (16.9)		
≤400	13 (52.0)	64 (83.1)		
CA19-9 (U/ml)			2.239	0.135
>35	3 (12.0)	3 (3.9)		
≤35	22 (88.0)	74 (96.1)		

81   * $P<0.05$

82   Values are represented as mean ± standard deviation or number (percentage).

83

84 **Supplementary Table 4** Comparison of qualitative MRI findings between CK19 negative and

85 positive HCCs in training set

MRI Features	CK19+ (n=25)	CK19- (n=77)	κ value	*P value*
Size			1.000	0.891
>5 cm	10（40）	32（41.6）		
≤5 cm	15（60）	45（58.4）		
Signal intensity on arterial phase			0.852（1）	0.013*
High	22（88）	77（100）		
Low/Iso	3（12）	0（0）		
Dynamic enhancement pattern			0.662（1）	0.432
Wash in and wash out	24（96）	76（98.7）		
Delayed enhancement	1（4）	1（1.3）		
Persistent enhancement	0	0		
No or slight enhencement	0	0		
Rim enhancement on arterial phase			0.731（8）	0.018*
Present	9（36）	11（14.3）		
Absent	16（64）	66（85.7）		
Intratumoral vessels on arterial phase			0.703（14）	0.483
Present	16（64）	55（71.4）		
Absent	9（36）	22（28.6）		
Peritumoral enhancement			0.762（12）	0.724
Present	11（44）	37（48.1）		
Absent	14（56）	40（51.9）		
Venous thrombus			1.000	0.796

9

MRI Features	CK19+ (n=25)	CK19- (n=77)	κ value	P value
Present	2 （8）	5 （6.5）		
Absent	23 （92）	72 （93.5）		
Bile duct involvement			0.928 （1）	0.242
Present	3 （12）	4 （5.2）		
Absent	22 （88）	73 （94.8）		
Lymph node enlargement			1.000	0.568*
Present	0 （0）	2 （2.6）		
Absent	25 （100）	75 （97.4）		
Intratumoral cystic or necrotic portion			0.709 （15）	0.914
Present	13 （52）	41 （53.2）		
Absent	12 （48）	36 （46.8）		
Intratumoral fat			0.787 （7）	0.181
Present	3 （12）	19 （24.7）		
Absent	22 （88）	58 （75.3）		
Intratumoral hemorrhage			0.708 （12）	0.654
Present	9 （36）	24 （31.2）		
Absent	16 （64）	53 （68.8）		
Tumor capsule			0.637 （23）	0.726
Complete	3 （12）	14 （18.2）		
Incomplete	12 （48）	37 （48.1）		
Absent	10 （40）	26 （33.8）		
Target sign on DWI			0.777 （8）	0.001*
Present	13 （52）	14 （18.2）		
Absent	12 （48）	63 （81.8）		

MRI Features	CK19+ (n=25)	CK19- (n=77)	κ value	*P value*
Peritumor hypointensity on HBP			0.726（14）	0.359
Present	11（44）	42（54.5）		
Absent	14（56）	35（45.5）		
Margin			0.832（10）	0.101
I	0（0）	9（11.7）		
II	7（28）	25（32.5）		
III	16（64）	42（54.5）		
IV	2（8）	1（1.3）		
Target sign on HBP			0.736（10）	0.005*
Present	12（48）	15（19.5）		
Absent	13（52）	62（80.5）		
Intratumoral septum on portal/transition phase			0.899（5）	0.092
Present	19（76）	44（57.1）		
Absent	6（24）	33（42.9）		

86   * *P*<0.05

87   Values are represented as mean ± standard deviation or number (percentage).

88   Data of κ value in parentheses are the number of discordant cases in each variable.

89